Solitons as probes of the structure of holographic superfluids

Solitons as probes of the structure of holographic superfluids

Ville Keränen[1,2]**, Esko Keski-Vakkuri**[1,2,5]**, Sean Nowling**[3]
and K P Yogendran[1,4]

[1] Helsinki Institute of Physics, PO Box 64, FIN-00014 University of Helsinki, Finland
[2] Department of Physics, PO Box 64, FIN-00014 University of Helsinki, Finland
[3] NORDITA Roslagstullsbacken 23, SE-106 91 Stockholm, Sweden
[4] IISER Mohali MGSIPAP Complex, Sector 26, Chandigarh 160019, India
E-mail: esko.keski-vakkuri@helsinki.fi

Abstract. The detailed features of solitons in holographic superfluids are discussed. Using solitons as probes, we study the behavior of holographic superfluids by varying the scaling dimension of the condensing operator and make a comparison to the Bose–Einstein condensate–Bardeen–Cooper–Schrieffer comparison phenomena. Further evidence of this analogy is provided by the behavior of the solitons' length scales as well as by the superfluid critical velocity.

[5] Author to whom any correspondence should be addressed.

Contents

1. Introduction

In recent years, there has been a great deal of interest in the study of superfluidity in ultracold Fermi gases. In the laboratory, one cools a gas of fermionic atoms to temperatures below a few microkelvins. By subjecting the system to a controllable external magnetic field, one can tune the interactions in the fermionic gas. Usually, what one finds is a crossover phenomenon. On one side of the range the system is described by condensed loosely bound Cooper pairs of fermions, whereas at the other end the fermions become very strongly bound and the system is effectively characterized as a condensate of a fundamental bosonic degree of freedom. These two extremes are separated by the unitarity point, where the systems do not have a simple description in terms of either simple bosons or fermions.

At zero temperature, precisely at the unitarity point, apart from the fermion density the system has no other length scale. This feature is of interest to holographic model building in string theory, where it has been discovered that some strongly coupled scale invariant theories have a dual description in terms of gravitational theories in asymptotically anti-de Sitter (AdS) spacetimes of one higher dimension.

One of the first holographic models for a superfluid was introduced in [1][6]. This is a relativistic $(2+1)$-dimensional superfluid described holographically using a gravitational theory in $(3+1)$ dimensions. Using classical gravity theory, one expects to reproduce a large N strong coupling limit of a dual $(2+1)$-dimensional system, which we often refer to as the (dual) field theory. Typically, one expects the field theory to possess both bosonic and fermionic degrees of freedom, and the operator responsible for symmetry breaking could then be a composite operator including fermions (see e.g. the discussion in [2]). It was shown in [1] that for low enough temperatures, the U(1) global symmetry of the field theory is broken and that this phase,

---

[6] The model was actually presented as a holographic model for some aspects of superconductivity, but a more precise interpretation is that of a superfluid.

in the dual gravity description, presents itself as a black hole with complex scalar hair outside its horizon.

It is important to consider the extent to which the model [1] can mimic the salient features of cold atomic systems. It is obvious that it cannot be literally interpreted as a model for such systems. The cold atoms are a $d = 3$ non-relativistic system, while the holographic system describes a relativistic $d = 2$ large N (mean-field[7]) theory. Furthermore, it would be natural to explore the possibility of finding a gravity dual for a system at unitarity in view of the conformal invariance of the gravity description. We will address the question as to whether there is any sense in which [1] could resemble such a system.

Firstly, it is encouraging to note that many of the features of the non-relativistic condensates are expected to have relativistic analogues, since the basic intuitions about the nature of bound states are the same [3]. Secondly, the unitarity regime was also studied without introducing a dimensionful parameter, using an ϵ-expansion [4, 5]. Further [4, 5], one way of interpreting the ϵ-expansion study of the unitarity regime is as a family of conformal field theories separating a Bardeen–Cooper–Schrieffer (BCS)-like unitarity phase (near $d = 2$) from a Bose–Einstein condensate (BEC)-like unitarity phase (near $d = 4$) with the most interesting and strongly coupled unitarity near $d = 3$. There is a natural parameter controlling the physics of the holographic condensates, namely the scaling dimension of the condensing operator. Changing the scaling dimension might be interpreted as a family of conformal field theories corresponding to different kinds of superfluids on the unitary regime, as in [4, 5][8]. Finally, we would like to point out that the authors of [3] found that, at least when approaching unitarity from the BEC side, relativistic and non-relativistic systems behave similarly.

The fact that this system is strongly coupled, involves both fermion and boson degrees of freedom, and may be studied using conformal field theory methods, suggests that it may have a degree of commonality with holographic theories [7–9]. To summarize, we adopt the point of view that the unitarity regime of cold atoms provides a nice guide to study, interpret and organize many of the features of the superfluid first described in [1], and probably other related models as well.

What, then, would be a suitable probe for the subtle microscopic features on both sides of unitarity? It is interesting to note that solitons in a superfluid phase provide nice probes of the short-distance structure, even at the mean-field level [10, 11] (at least away from the strict unitarity limit, where constructing the mean-field theory is problematic). The main reason for this is that across the soliton's core the superfluid must interpolate all the way from the broken to the symmetry restored phase. The core's structure will have features that may be used to characterize the short-distance features of the theory[9]. An interesting example of the use of solitons in understanding the microscopic constituents of certain supersymmetric quantum field theories may be found in [12].

---

[7] We use the phrase 'mean field' in the sense of expanding around a ground state, which is not necessarily the Gaussian one. The classical gravity solution, provided it is stable, defines a saddle point for a perturbative expansion that maps into a perturbation expansion on the field theory side. While the elements of expansion are not identical across the two descriptions, they are nevertheless corresponding.

[8] The analogy between our family of fixed points and the one in [4, 5] cannot be taken too literally since in [4, 5] (see also [6]) the condensate scaling dimension is kept fixed while ϵ is varied.

[9] To our knowledge, such an exploration of solitonic features has not been conducted in the context of an ϵ-expansion approach.

As will be described, solitons in the holographic system possess several similarities to solitons found in cold atomic systems. In addition, we will find that the analogy to atomic systems is useful for organizing certain linear response calculations in the holographic system. Conversely, the properties of holographic solitons may be of interest for the study of their real-world counterparts. Holographic duals provide a rather simple and effective theory for a strongly coupled system at finite temperature. In the case of superfluids, they give a toy model for the condensate and the normal component and their interactions. For example, we can study how the charge depletion at the core of the soliton varies as a function of the temperature, which would be very difficult using standard condensed matter techniques.

2. One holographic model of superfluidity

Hartnoll *et al* [1] constructed a holographic dual for a superfluid in $(2+1)$ dimensions, provided by an Einstein–Abelian–Higgs system in $(3+1)$-dimensional asymptotically AdS space,

$$S_{AdS} = \int d^4x \sqrt{-g} \left[\frac{1}{\kappa_4^2} \left(\mathcal{R} + \frac{6}{L^2} \right) - \frac{1}{q^2} \left(|D_\mu \Psi|^2 + m^2 |\Psi|^2 + \frac{1}{4} F_{\mu\nu}^2 \right) \right]. \quad (1)$$

By virtue of the AdS/CFT correspondence[10], gauged symmetries of the gravitational (bulk) theory correspond to global symmetries of the dual-field theory (which shall also be called the 'boundary theory'). Thus, the Lorentz covariance of the boundary theory follows from the bulk diffeomorphism invariance and the bulk U(1) gauge symmetry gives rise to a U(1) global symmetry in the dual-field theory. We shall identify the corresponding conserved charge with the particle number in the language appropriate for atomic systems.

Spontaneous breakdown of this global symmetry will then result in a charged superfluid condensate. The formation of the condensate is dual, in the bulk gravitational theory, to spontaneous gauge symmetry breaking—that is to say, to the condensation of a scalar field charged under the gauge symmetry. The entire system may be placed at finite temperature by including a black hole background, in which case the Hawking temperature corresponds to the equilibrium temperature of the superfluid.

Basic properties of superfluids, such as transport properties at the linearized level [13–17], have been studied using the action (1); the derivation of nonlinear superfluid dynamics has been discussed in [18].

The AdS–CFT dictionary tells us that the gravitational action in four dimensions evaluated on the solutions to the equations of motion (with suitable boundary conditions) is the generating functional of various moments of the corresponding operators in the $(2+1)$-dimensional quantum field theory

$$e^{-S_{AdS}(onshell)} = \langle e^{-\int d^3x (\rho(x)\mu(x) + \mathcal{O}(x)J(x))} \rangle_{QFT}. \quad (2)$$

The metric of the bulk spacetime is required to asymptote to AdS space (the asymptotic behavior in fact defines the energy momentum tensor of the field theory). The boundary CFT operators are related to the behavior of the bulk fields in the asymptotically AdS regime $z \to 0$. In this region,

[10] The precise version of this correspondence states that a conformal field theory (CFT) in flat space is dual (in the sense of strong coupling) to a string theory on AdS space. In this paper we use the term CFT to refer to the dual-field theory that may or may not be conformal.

the solutions of the equations of motion for the bulk fields may be expanded in a Frobenius-type power series in z

$$A_t(x, z) = \mu(x) + z\rho(x) + \cdots, \tag{3}$$

$$\Psi(x, z) = z^\Delta \langle \mathcal{O}_\Delta(x) \rangle + z^{\Delta+2} \mathcal{F}_1(x) + \cdots + z^{3-\Delta} J(x) + z^{5-\Delta} J_1(x) \cdots,$$

where the ellipses in (3) denote terms with higher powers of z in the two series and the mass of the bulk field Ψ is

$$m^2 = \Delta(\Delta - 3). \tag{4}$$

In the dual-field theory, one identifies $J(x)$ with the source for the operator $\mathcal{O}_\Delta$ of scaling dimension Δ in the dual-field theory. The c-number $\langle \mathcal{O}_\Delta(x) \rangle$ occurring in (3) is identified with the expectation value of the dual operator given an external source, $J(x)$. Also, $\mu(x)$ is interpreted as a chemical potential in the dual-field theory, while $\rho(x)$ is the (canonically) conjugate variable, the charge (or particle number) density.

To have a well-defined solution, one must impose boundary conditions that fix the value of $J(x)$ in the gravitational theory. The value of $\mathcal{O}_\Delta(x)$ is then determined uniquely. In the remainder of the paper, we choose our units so that the AdS scale is fixed to $L = 1$. For large m^2, one finds a solution only if Δ is chosen to be the largest root of (4). However, for[11]

$$-\frac{9}{4} < m^2 < -\frac{5}{4}, \tag{5}$$

one obtains a sensible solution using either root of (4) (for a discussion, see e.g. [20]). In the window of two quantizations, there are two field theories with operators of different scaling dimensions, corresponding to the choice of boundary conditions.

To construct a holographic superfluid, one must search for solutions to the equations of motion obtained from (1) such that the charged operator has a nonzero expectation value even after its external source is removed. Gravitationally, this means that one is searching for a black hole solution with scalar hair in asymptotically AdS space. In Minkowski space, such hairy black holes do not exist, but in [21] it was noted that the negative cosmological constant may stabilize hair outside a black hole.

Throughout this paper, we work in the so-called probe limit ($\frac{\kappa_4^2}{q^2}$ is small), so that the backreaction to gravity can be ignored. The gravitational solution involves a planar AdS–Schwarzschild metric,

$$ds^2 = \frac{1}{z^2}(-f(z)\,dt^2 + f(z)^{-1}\,dz^2 + dr^2 + r^2\,d\theta^2), \tag{6}$$

where $f(z) = 1 - z^3$. In the above, temperature has been absorbed in a rescaling to dimensionless coordinates. After the rescaling, the only free parameter is the dimensionless ratio μ/T. Changing this ratio may be thought of as changing the temperature (chemical potential) and keeping the chemical potential (temperature) fixed. In this background, charged scalar hair may then emerge depending on the temperature.

When studying homogeneous states it is possible to go beyond the probe approximation and include back reaction from the bulk scalar and gauge fields to the black hole metric [22]. In doing so, one verifies that working with an uncharged black hole is a good approximation when the scalar field's charge is large ($\frac{\kappa_4}{q} \sim 0.01$) and mass is small.

[11] We recall that masses in AdS spacetimes are permitted to be slightly negative ($m^2 > -9/4$) without triggering an instability so long as they are above the Breitenlohner–Freedman (BF) bound [19].
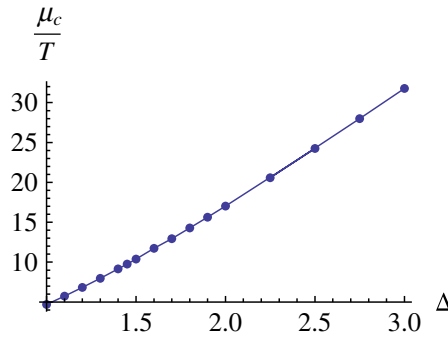
Figure 1. The critical value of the chemical potential as a function of the charged operator's scaling dimension, while keeping the temperature fixed. $\Delta_-(\Delta_+)$ is to the left (to the right) of 1.5 on the horizontal axis.

To find the dual-field theory operator expectation values, we need to solve the classical equations of motion in AdS space to obtain the on-shell fields. In the probe approximation, the equations of motion become

$$0 = \frac{1}{\sqrt{-g}} \partial_\mu (\sqrt{-g} g^{\mu\nu} \partial_\nu R) + m^2 R - R(\partial_\mu \chi - A_\mu)^2, \tag{7}$$

$$0 = \frac{1}{\sqrt{-g}} \partial_\mu (\sqrt{-g} F^{\mu\nu}) - R^2 (A^\nu - \partial^\nu \chi), \tag{8}$$

$$0 = \partial_\mu (\sqrt{-g} R^2 g^{\mu\nu} (\partial_\nu \chi - A_\nu)), \tag{9}$$

where we have defined the real valued fields R and χ according to the relation $\Psi = \frac{1}{\sqrt{2}} R e^{i\chi}$.

The scalar fields are unstable to spontaneous symmetry breaking as one raises the chemical potential μ, so that above the critical value μ_c the boundary theory enters the superfluid phase. As we vary the mass of the bulk scalar field over the range (5), we cover the following range of scaling dimensions: $\frac{1}{2} < \Delta_- \leqslant \frac{3}{2}$; $\frac{3}{2} \leqslant \Delta_+ < \frac{5}{2}$. Higher masses then correspond to the range $5/2 \leqslant \Delta_+$.

One effect of the varying scaling dimension is a change in the critical value μ_c of the chemical potential where the superfluid transition happens. In figure 1, we have plotted μ_c as a function of Δ. We see that operators of larger scaling dimension have larger (smaller) values of μ_c (T_c).

3. Solitons as a way of studying the properties of the superfluid

The last section described a set of holographic superfluids that may be obtained by varying the scaling dimension and chemical potential. There are many quantities that one could study: for example, the chemical potential dependence of the superfluid order parameter near the critical temperature first found in [23],

$$\langle \mathcal{O}_\Delta \rangle \sim \sqrt{\frac{\mu}{\mu_c} - 1}. \tag{10}$$

A key question is: what does one learn about the superfluids from such computations? For example, the last scaling is presumably a mean field result. For instance, one would like to know how to characterize the degrees of freedom that are the constituents of the superfluid (since this is far from obvious in the holographic description).

There are at least three routes that one might consider. The obvious one is to come up with a detailed top-down model, with complete control over the boundary theory at the microscopic level, as in the original case of $D3$-branes and $N = 4$ super-Yang–Mills theory (for papers in this direction, see [2, 24, 25]). However, most models are of the bottom-up type, where the fundamental degrees of freedom and dynamics of the boundary theory are unknown. That leaves us two other strategies to consider.

The first is to consider linear response theory. It is straightforward to study the linear response of fields already involved in the gravity solution, but one is also interested in the way other fields, such as fermions, might respond to the superfluid. This approach is obstructed because a bottom-up approach generally lacks a stringy embedding that would dictate the allowed fermions.

The second, especially clean, way to study holographic superfluids is to study kinks and vortex solutions that asymptote to the homogeneous ground states described in section 2. The key reason is that it is known that kinks and vortices may shed light on the short-distance features, even at the mean-field level. Essentially this is because the core region must interpolate all the way to the symmetric phase and hence the soliton must know about the physics of all length scales. Because one expects mean-field theory to still be sufficient, it is enough to look for inhomogeneous solutions to classical gravity. An advantage of spatially dependent solutions is that they are inherent to the system—one does not need to turn on any external fields to excite it.

In the rest of this section, we discuss how to construct solitonic solutions to the gravitational equations of motion. Then we discuss several features of the solitons found in [26–28] and an analogy to BEC–BCS, which is useful both for organizing the holographic results and for suggesting further tests one might perform.

3.1. The method

The differential equations obtained from (1) are a set of coupled nonlinear partial differential equations that are approached most easily numerically. The basic strategy will be to exploit the fact that the equations are elliptic outside the horizon. This will allow us to construct an auxiliary heat equation that we solve numerically[12].

In more detail, as discussed in [28], when we work in the $A_z = 0$ gauge and use the cylindrical symmetry the equations of motion may be brought to the following form for vortex

---

[12] It is instructive to recall how one might solve the Poisson equation

$$\nabla^2 \phi = 0, \tag{11}$$

by studying a heat equation

$$(\partial_\tau + \nabla^2)\phi(\tau, x). \tag{12}$$

Starting with any reasonable initial field configuration, the evolution is such that at late times the field configuration 'flows' to the 'nearest' configuration, satisfying (11). In this case, nearest means in the same topological class.
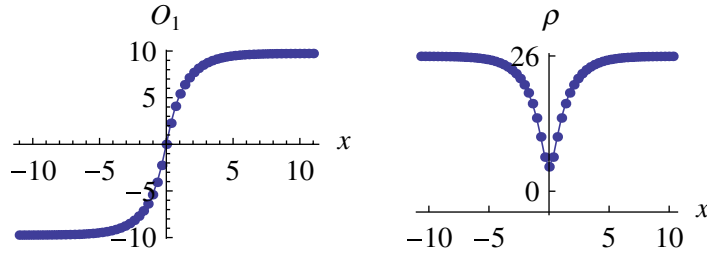
Figure 2. A typical kink soliton profile as computed using holography. On the left is the condensate's profile plotted in the transverse coordinate. On the right is the density profile in the same transverse direction. These curves were obtained using a $\Delta = 1$ condensate.

configurations:

$$0 = f\partial_z^2 \tilde{R} + \left(\partial_z f + (2\Delta_- - 2)\frac{f}{z}\right)\partial_z \tilde{R} - \Delta_-^2 z\tilde{R} + \frac{1}{r}\partial_r(r\partial_r \tilde{R}) - \tilde{R}\left(-\frac{1}{f}A_t^2 + \frac{(A_\theta - n)^2}{r^2}\right),$$

$$0 = f\partial_z^2 A_t + \frac{1}{r}\partial_r(r\partial_r A_t) - z^{2\Delta_-}\tilde{R}^2 A_t, \tag{13}$$

$$0 = \partial_z(f\partial_z A_\theta) + r\partial_r\left(\frac{1}{r}\partial_r A_\theta\right) - z^{2\Delta_-}\tilde{R}^2(A_\theta - n),$$

where we have defined $\tilde{R} = z^{-\Delta_-}R$. A similar set of equations may be obtained for kink solutions as described in [27] for the case of $m^2 = -2$.

For both vortex and kink solutions we impose regularity conditions at the horizon. This is the same condition as that used to find the homogeneous solution and is necessary for obtaining a steady-state solution. In the asymptotically AdS region, we will impose a uniform chemical potential as well as a vanishing scalar non-normalizable mode. The vortex solution also involves the θ component of the gauge field, which we take to vanish at the AdS boundary. This corresponds to having no external driving vorticity to source the vortex.

The basic strategy for finding solutions is to make an initial guess at a solution (that respects the boundary conditions) and then let this guess flow according to an auxiliary heat equation. By waiting for long enough in auxiliary time, we arrive at a solution of the equations of motion (13). In reality all this is done on a lattice and one stops the simulation when the evolution is suitably slow. For details of the algorithm as well as error analysis, see [26]. Typical kink and vortex solutions are shown in figures 2 and 4.

With this method we find that we are able to obtain good numerical solutions for values of $T/T_c > .5$ (or $\mu/\mu_c < 2$). See [27] for a detailed discussion of the numerics. The numerical computations were performed with MATHEMATICA and some simple C-programming using desktop computers.

3.1.1. Solutions. Kinks. In figure 2, we have plotted a typical kink solution. We see that the condensate passes through zero, as required by topology and continuity. We also see that the (number) density does not completely vanish in the core of the soliton. A nice feature of the holographic model is that it gives an effective theory for the condensate *and* thermal fluctuations, so one can easily study the effects of varying temperature. In order to disentangle
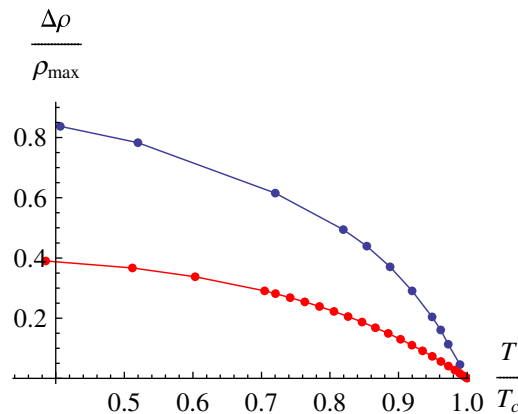
Figure 3. The core charge depletion fraction for kink solitons at $m^2 = -2$ for varying T/T_c. $\Delta = 1$ is indicated by the blue curve (top) and $\Delta = 2$ is indicated by the red curve (bottom). Reproduced from [27]. Copyright 2010 by the American Physical Society.
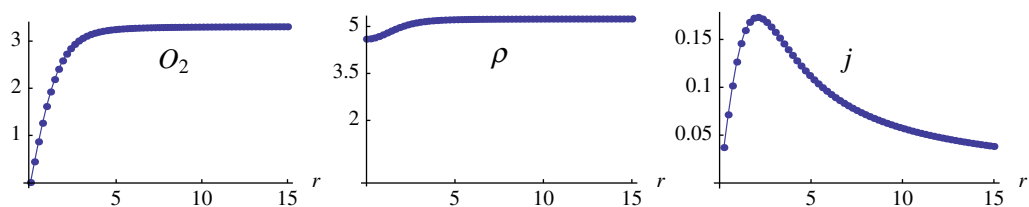

Figure 4. A typical vortex soliton profile as computed using holography. On the left is the condensate's radial profile. In the middle is the profile of the charge density. On the right is the current density's radial profile. These curves were obtained using a $\Delta = 2$ condensate.

the thermal fluctuations, we reproduce figure 3 from [27] displaying the charge density's core depletion as a function of the temperature. This graph indicates that the two superfluids have very different behavior as one lowers the temperature. Specifically, one finds that the $\Delta = 2$ superfluid has an excess of charge density lying in its solitons' cores, in addition to the condensate's contribution. This latter feature is totally different from what one would obtain from a simple Gross–Pitaevskii picture for a purely bosonic condensate at zero temperature, where the density goes to zero at the core.

Vortices. In figure 4, we have shown a typical vortex profile. Again, we find that the condensate vanishes in the vortex's core, as expected. We also find that the charge density does not typically vanish in the core. Finally, as discussed in [28], we may identify the superfluid current from the angular component of the bulk gauge field. The superfluid current rises from zero at infinity until the critical velocity is surpassed and then falls to zero because the core is in the normal phase.

As for the kink solutions, we can again easily study the effect of varying temperature. We have reproduced figure 5 from [28] showing the temperature dependence of the core charge depletion fraction. This figure also clearly shows that the $\Delta = 2$ fluid has an 'excess' charge density in its core as compared to the $\Delta = 1$ fluid. In the next section, we recall what happens in the BEC–BCS crossover. This will serve as a useful guide to help interpret the core features of holographic solitons.
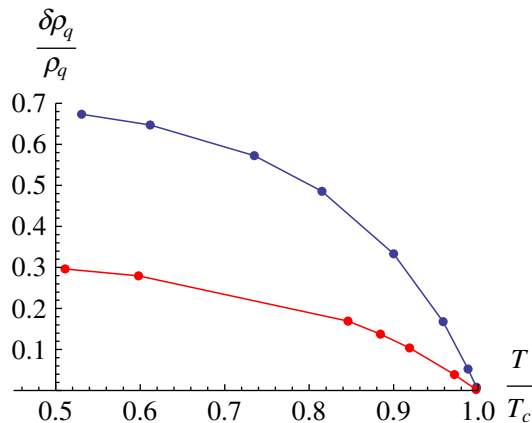
Figure 5. The core charge depletion fraction for vortex solitons at $m^2 = -2$ for varying T/T_c. $\Delta = 1$ is indicated by the blue curve (top) and $\Delta = 2$ is indicated by the red curve (bottom). Reproduced from [28]. Copyright 2010 by the American Physical Society.

3.2. The Bose–Einstein condensate (BEC)–Bardeen–Cooper–Schrieffer (BCS) analogy

In the last section, we saw that when $m^2 = -2$, solitons have very different core features when one changes the scaling dimension of the condensing operator. In this section, we wish to use the BEC–BCS crossover as a benchmark system to help us organize our holographic results. This will help us both to interpret the features of the holographic solitons and to suggest further questions.

For the non-relativistic BEC–BCS crossover at zero temperature, the authors of [10, 11] have studied the behavior of kink and vortex solitons. In both papers, it was found that soliton cores in fermionic superfluids have non-vanishing number densities of cold atoms, even though the condensates vanish. This is very different from BEC solitons, where the atomic number density vanishes (at zero temperature) when the condensate vanishes. In these systems, soliton cores are able to reveal the microscopic structure to the superfluid, even at the mean-field level. For fermionic superfluids, as one approaches the cores, there are additional states available in the form of fermion excitations because the core is in the normal phase. On the other hand, bosonic superfluid solitons have vanishing core atomic number densities because there are no additional non-condensate states available at zero temperature. In these papers, it was also found that the core structures interpolated smoothly between the BEC and BCS limits. At finite temperature, even in the BEC superfluid, we expect that there will be a small contribution to the number density from the thermal cloud (non-condensate normal fluid component) which can show up in the soliton's core.

In both [10, 11], it was argued that the solitonic cores were also able to reveal the character of the additional states carried by a fermionic superfluid's core. Specifically, in [10] it was found that the solitons display Friedel oscillations in their cores. In [11], it was found that the oscillations in vortices were finite size effects, not Friedel oscillations. On the other hand [11] found that the vortex was sensitive to k_f through the fact that the vortices had different length scales in the cores and tails.

Comparing the holographic superfluids to the crossover systems suggests that we should interpret excess core charge density in a soliton as a sign that there are additional
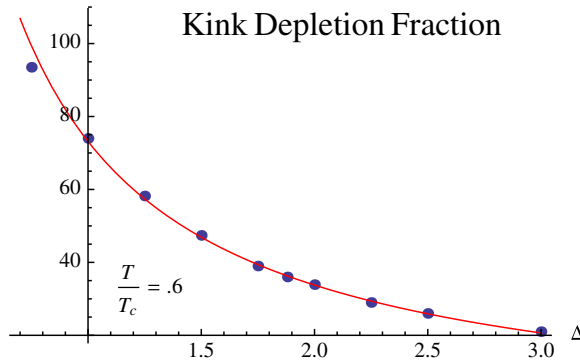
Figure 6. The charge-density depletion fraction ($\times 100$) for kink solitons as a function of the condensate's scaling dimension at $T/T_c = 0.6$. The curve is a best fit obtained for scaling dimensions above the BF bound ($\Delta = 3/2$).

non-condensate states residing in the core. Therefore, we might expect to see that one can interpolate between 'empty' and 'full' cores as one changes the gravitational mass parameter, hence changing the scaling dimension [4, 5]. In addition, we could try to use these holographic solitons to identify the fermionic/bosonic character of the 'excess' states in the soliton's core. To do this, there are at least two ways to proceed. Firstly, one may try to identify whether vortices display single or multiple length scales in their cores and tails. Secondly, one could hope to identify any Friedel oscillations.

3.3. Varying the scaling dimension

In subsection 3.2 it was pointed out that comparison to the crossover indicates that one should expect the charge-density depletion fraction in a soliton's core to interpolate between 0 and 100% as one varies the scaling dimension of the condensing operator (at zero temperature). In principle, it is simple to repeat the analysis in subsection 3.1 when $m^2 = -2$, now allowing for more general scaling dimensions. In practice, one cannot work at zero temperature for two reasons. Firstly, we have assumed a probe approximation that is only valid for temperatures moderately below T_c (μ above μ_c). Secondly, even if we went beyond the probe approximation, it is computationally too expensive to obtain solutions for arbitrarily low temperatures.

In order to proceed, we note that in figures 3 and 5 the depletion fraction seems to be saturating near $T/T_c \sim 0.5$, independently of the scaling dimension. Therefore, as an approximation to the depletion fraction at low temperature, we will study solitons at $T/T_c = 0.6$ as we vary Δ. Finally, for the sake of brevity we will focus on the kink solitons. It is a straightforward exercise to show that vortices also display the same features as one varies Δ.

In figure 6, we see the smoothly varying charge-density depletion fraction in the core of a kink soliton at fixed $T/T_c = .6$. A numerical fit of the form

$$\frac{\delta\rho}{\rho_{\max}} = A + \frac{B}{\Delta} \tag{14}$$

was made for the points with scaling dimension greater than $\Delta = 3/2$. The best fit values are $(A, B) = (-0.06, 0.8)$. The small variation in the graph is primarily due to the small uncertainty in the value of T/T_c. We note that there is a visible change in the behavior of the depletion
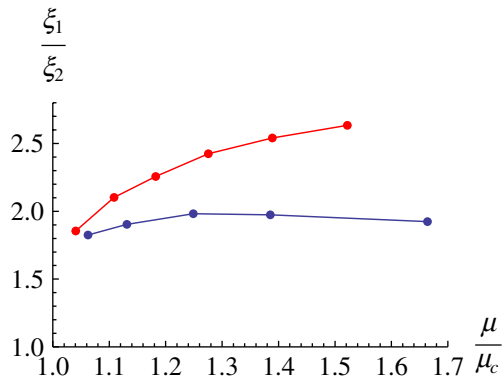
IOP Institute of Physics ΦDEUTSCHE PHYSIKALISCHE GESELLSCHAFT

Figure 7. Here we have reproduced the graph from [28] plotting the ratio of length scales of variation as determined from the condensates profile for vortex solutions. The blue curve (bottom) indicates a $\Delta = 1$ condensate and the red curve (top) indicates a $\Delta = 2$ condensate. Copyright 2010 by the American Physical Society.

fraction as one lowers Δ, presumably saturating close to 100% at $\Delta \sim 1/2$, although these values are beyond what we can currently simulate.

4. Characterizing the core states

4.1. Multiple length scales

Having seen that one can indeed control a soliton's core charge depletion fraction by varying the condensing operator's scaling dimension, and hence the number of states available in the soliton's core, we would also like to see to what extent one may try to characterize these states. The simplest way one might do this is to obtain characteristic length scales for the condensate's profile in the core and in the asymptotic tails. In [11], it was found that bosonic superfluids essentially have one length scale, while fermionic superfluids lead to distinct length scales in the two regimes. We may try to identify how dissimilar the soliton's length scales are according to how their ratio varies as a function of μ for different operator scaling dimensions. Figure 7 shows the graph obtained in [28] and indicates that there are two distinct length scales as one increases the scaling dimension. It would be very interesting to see what happens to the corresponding graph for $\Delta \sim 1/2$, the lowest allowed value. The comparison with the crossover would predict that in this regime the corresponding curve would be completely flat. Unfortunately, we do not have resources to say more about this value of Δ. In subsection 4, we will discuss critical velocities obtained from linear response theory. Comparison of these critical velocities to the superfluid's sound modes will lead to a qualitatively similar comparison to figure 7.

4.2. Friedel oscillations

A final feature of solitons in the crossover was the possible observation of Friedel oscillations. As discussed in [27, 28], we found no evidence of Friedel oscillations in the holographic solitons. One possible reason for the absence of the oscillations, if they existed, is that they may have been obscured by too large a temperature or suppressed in the $\frac{1}{N}$ expansion.

4.3. Critical velocity

Another way to probe the constituents of a superfluid is to study superfluid flows. As one increases the velocity of the flow, it becomes energetically more favorable for the superfluid to radiate quasiparticles and go to the normal phase. The velocity at which this happens is called the critical superfluid velocity. It is possible to estimate the critical velocity using a simple kinematical argument due to Landau. According to Landau's criterion, the critical superfluid velocity is given by the formula

$$v_c = \min_k \frac{\epsilon(k)}{k},\tag{15}$$

where $\epsilon(k)$ is the quasiparticle dispersion relation in the superfluid and the minimum is taken over all the quasiparticles. Strictly speaking, the Landau criterion only gives an upper bound for the critical velocity and indeed at finite temperature one expects to see a smaller critical velocity than the Landau criterion tells us [29]. However, the Landau criterion can still act as a useful guide in estimating the critical velocities.

For a BCS superfluid, the critical velocity is set by the lightest fermionic excitations, which leads to an estimate

$$v_c^{\text{BCS}} \approx \frac{\omega_{\text{gap}}}{k_f},\tag{16}$$

where k_f is the Fermi momentum and ω_{gap} is the energy gap for fermions in the superfluid phase. On the other hand, on a BEC superfluid the critical velocity is set by the sound modes with lowest sound velocity v_s so that

$$v_c^{\text{BEC}} \approx v_s.\tag{17}$$

Unfortunately, in the holographic superfluid model we do not have direct access to possible fermions in the system without adding extra fields to the bulk. Even though one can access some fermionic features of the system by adding probe fermions to the bulk, the connection of these fermions with those possibly comprising the condensate is not very clear. Thus, we are unable to calculate the fermion dispersion relations required for obtaining the 'fermionic' Landau criterion.

Instead, we can calculate sound velocities and compare them to the critical velocity obtained from the vortex solutions. A study of the Landau criterion in the BEC–BCS crossover can be found in [30].

According to [15], the second sound has the lowest sound velocity, at least in the part of parameter space studied there. As shown in [13], the second sound can be calculated from thermodynamic quantities as

$$v_2^2 = -\frac{(\partial^2 P/\partial \xi^2)_{\mu,T}}{(\partial^2 P/\partial \mu^2)_{\xi,T}}.\tag{18}$$

Here, $\xi = \nabla \chi$, where χ is the phase of the condensate and the thermodynamic derivatives are evaluated at $\xi = 0$. More details of the calculation may be found in [13].

The critical superfluid velocity may be obtained from the vortices, as described in [28]. One simply looks for the radial position ρ_* inside the vortex where the condensate vanishes and evaluates the superfluid velocity at that radius. This leads to

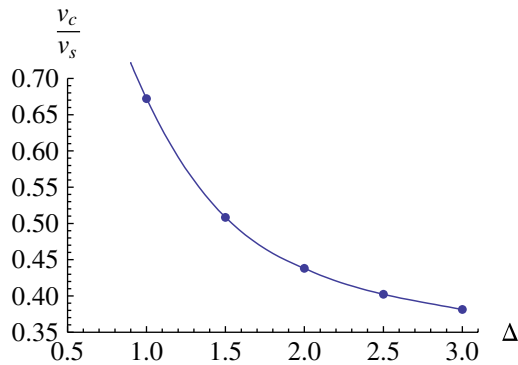$$v_c = \frac{1}{\mu} \frac{n}{\rho_*}.\tag{19}$$

Figure 8. The ratio of the critical superfluid velocity and the second sound velocity as a function of the condensate scaling dimension. The curve in the figure is an interpolating function, while the dots are the real data points.

A convenient way of determining ρ_* is to identify it with the position of peak current [11, 28].

The ratio of the vortex critical velocity to the sound velocity is plotted in figure 8 for $T/T_c \approx 0.7$. We find that the ratio of the two velocities seems to be approaching 1 as the scaling dimension of the condensing operator is lowered, and is notably smaller than 1 as the dimension is larger. In a BEC-like superfluid one would expect a sound mode to determine the critical velocity. Recalling that in our crossover analogue the small scaling dimensions correspond to the supposed BEC region, we indeed find a consistent picture with the analogue. In a BCS-like superfluid one expects the critical velocity to be set by a fermionic excitation rather than a sound mode. Indeed it seems that in the supposed BCS region the critical velocity is probably set by something other than a sound mode.

5. Discussion

The possibility of applying holographic techniques to low-dimensional systems is an exciting recent development in string theory. However, because the set of quantities that are readily computable are typically quite different, it can be difficult to develop necessary model building intuitions. For this purpose, it is often useful to compare holographic constructions to known real-world systems that display many features expected of holographic systems. In this paper, we have focused on using the BEC–BCS crossover as a guide to features observed in holographically constructed superfluids. This is a crossover from a system of fundamental bosons to fundamental fermions, both of which may display superfluidity. Most relevant for holography, this is a system that is strongly interacting and may be studied by moving along a family of fixed points [6].

We began by constructing kink and vortex solitons in holographic superfluids obtained by condensing operators of scaling dimensions $\Delta = 1$ and 2. Surprisingly, their cores display different features, with the $\Delta = 2$ soliton cores supporting much larger charge densities.

Similar features occur in the BEC–BCS crossover, where there are additional non-condensate states available away from the BEC regime. In this setting, the additional states are comprised of pre-formed bosons and fermions. Also, the solitons 'know' about the fermions

in the BCS regime because the Fermi momenta control the core size as well as any Friedel oscillations.

Comparison with the crossover physics suggested that as we vary the condensing operator's scaling dimension, we should expect the core features to smoothly interpolate as we move along the family of CFTs. Indeed, this is precisely what was obtained. As we increased the scaling dimension, the amount of charge supported by soliton cores increased monotonically. Also consistent with this trend is the fact that the difference between core and tail length scales of variation increases with Δ [28]. Finally, from the solitons we find no signature of Friedel oscillations for $T/T_c > .5$.

In an effort to understand the character of the excess charged states available in soliton cores, we also compared the critical velocity obtained from vortex cores to the Landau critical velocity. As one lowers Δ the vortex critical velocity approaches the Landau critical velocity monotonically. This is what one would expect for a BEC superfluid.

The BEC–BCS analogy may also be used to explain the results found in [23] for conductivities calculated on the superfluid phase. There it was found that there are delta function-like spikes on the frequency-dependent conductivity. These spikes were interpreted as being due to bound states. The only bound states that may contribute to the conductivity (current–current correlator) are those that have a vanishing net charge. Thus, a natural candidate for the spikes on the BEC–BCS picture is a bound state of a fermion–hole pair. Such pairs should exist on the BCS side only. Indeed it was found in [23] that the spikes appear on the 'large' scaling dimension side, and the binding energy calculated from the position of the spikes seems to increase as the scaling dimension is lowered. This is consistent with the crossover picture where the interactions increase as one approaches unitarity from the BCS side. Holographically, as one moves across the BF bound ($\Delta = 3/2$) to lower scaling dimensions, at some point the spikes disappear, which would seem to signal that the bound state disappears. This fits well with the BEC–BCS analogy since on the BEC side (the low scaling dimensions) the Fermi surface and light fermionic excitations are expected to completely vanish. The crossover analogy would naturally explain why the particle–hole bound state would go away.

We have shown that the BEC–BCS may be a useful guide to holographic superfluids, owing to their common strong coupling and conformal features. They also share common structures in their solitons. However, to make the crossover more than an interpretational guide it would be more convincing if there was a direct signature of fermionic features in holographic superfluids. There are at least two places one might hope to find such features. First, if one could cool solitons to low enough temperatures it might be possible to observe Friedel oscillations. This would be an unambiguous signal. A second route would be to try to have a better understanding of fermion probe calculations, with the hope that they could reveal any fermionic feature encoded in the bulk geometry.

Acknowledgments

IOP Institute of Physics ⊕ DEUTSCHE PHYSIKALISCHE GESELLSCHAFT

References

[1] Hartnoll S A, Herzog C P and Horowitz G T 2008 *Phys. Rev. Lett.* **101** 031601 (arXiv:0803.3295 [hep-th])
[2] Gubser S S *et al* 2009 *Phys. Rev. Lett.* **103** 141601 (arXiv:0907.3510 [hep-th])
[3] Nishida Y and Abuki H 2005 *Phys. Rev.* D **72** 096004 (arXiv:hep-ph/0504083)
[4] Nishida Y and Son D T 2006 *Phys. Rev. Lett.* **97** 050403 (arXiv:cond-mat/0604500)
[5] Nishida Y and Son D T 2006 *Phys. Rev.* A **75** 063617 (arXiv:cond-mat/0607835)
[6] Nikolic P and Sachdev S 2007 *Phys. Rev.* A **75** 033608 (arXiv:cond-mat/0609106)
[7] Nishida Y and Son D T 2007 *Phys. Rev.* D **76** 086004 (arXiv:0706.3746 [hep-th])
[8] Son D T 2008 *Phys. Rev.* D **78** 046003 (arXiv:0804.3972 [hep-th])
[9] Balasubramanian K and McGreevy J 2008 *Phys. Rev. Lett.* **101** 061601 (arXiv:0804.4053 [hep-th])
[10] Antezza M, Dalfovo F, Pitaevskii L P and Stringari S 2007 *Phys. Rev.* A **76** 043610 (arXiv:0706.0601)
[11] Sensarma R, Randeria M and Ho T L 2006 *Phys. Rev. Lett.* **96** 090403 (arXiv:cond-mat/0510761)
[12] Collie B and Tong D 2009 *J. High Energy Phys.* JHEP08(2009)006 (arXiv:0905.2267 [hep-th])
[13] Herzog C P, Kovtun P K and Son D T 2009 *Phys. Rev.* D **79** 066002 (arXiv:0809.4870 [hep-th])
[14] Basu P, Mukherjee A and Shieh H-H 2009 *Phys. Rev.* D **79** 045010 (arXiv:0809.4494 [hep-th])
[15] Herzog C P and Yarom A 2009 *Phys. Rev.* D **80** 106002 (arXiv:0906.4810 [hep-th])
[16] Yarom A 2009 *J. High Energy Phys.* JHEP07(2009)070 (arXiv:0903.1353 [hep-th])
[17] Amado I, Kaminski M and Landsteiner K 2009 *J. High Energy Phys.* JHEP05(2009)021 (arXiv:0903.2209 [hep-th])
[18] Sonner J and Withers B 2010 *Phys. Rev.* D **82** 026001 (arXiv:1004.2707 [hep-th])
[19] Breitenlohner P and Freedman D Z 1982 *Ann. Phys.* **144** 249
[20] Balasubramanian V, Kraus P and Lawrence A E 1999 *Phys. Rev.* D **59** 046003 (arXiv:hep-th/9805171)
[21] Gubser S S 2008 *Phys. Rev.* D **78** 065034 (arXiv:0801.2977 [hep-th])
[22] Horowitz G T and Roberts M M 2009 *J. High Energy Phys.* JHEP11(2009)015 (arXiv:0908.3677 [hep-th])
[23] Horowitz G T and Roberts M M 2008 *Phys. Rev.* D **78** 126008 (arXiv:0810.1077 [hep-th])
[24] Gauntlett J P, Sonner J and Wiseman T 2009 *Phys. Rev. Lett.* **103** 151601 (arXiv:0907.3796 [hep-th])
[25] Gauntlett J P, Sonner J and Wiseman T 2010 *J. High Energy Phys.* JHEP02(2010)060 (arXiv:0912.0512 [hep-th])
[26] Keranen V, Keski-Vakkuri E, Nowling S and Yogendran K P 2009 *Phys. Rev.* D **80** 121901 (arXiv:0906.5217 [hep-th])
[27] Keranen V, Keski-Vakkuri E, Nowling S and Yogendran K P 2010 *Phys. Rev.* D **81** 126011 (arXiv:0911.1866 [hep-th])
[28] Keranen V *et al* 2010 *Phys. Rev.* D **81** 126012 (arXiv:0912.4280 [hep-th])
[29] Navez P and Graham R 2006 *Phys. Rev.* A **73** 043612
[30] Diener R B, Sensarma R and Randeria M 2008 *Phys. Rev.* A **77** 023626 (arXiv:0709.2653v2 [cond-mat])